



ISSN: 2230-9926

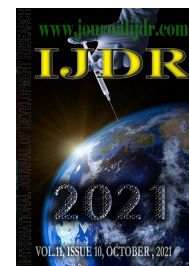
Available online at <http://www.journalijdr.com>

IJDR

International Journal of Development Research

Vol. 11, Issue, 10, pp. 50668-50675, October, 2021

<https://doi.org/10.37118/ijdr.22965.10.2021>



RESEARCH ARTICLE

OPEN ACCESS

MANUFACTURING AND PROCESSING OF AA3303 ALUMINUM ALLOY BY SYNTHESIS OF ELEMENTARY POWDERS BY POWDER METALLURGY TECHNIQUES OF HIGH ENERGY BALL MILLING AND HOT EXTRUSION

Moisés Euclides da Silva Junior¹, Diogo Monteiro do Nascimento¹, Enéas Carlos de Oliveira Silva¹, Inaldo Amorim da Silva², Tarsila Tenório Luna da Silva¹, Rafael Silva de Santana³ and Oscar Olimpio de Araujo Filho¹

¹Mechanical Engineering Department, Federal University of Pernambuco, Cidade Universitária, Recife 50740-540

²Design department, Federal Institute of Pernambuco, Av. Prof. Luís Freire, 500, Cidade Universitária, Recife 50740-545

³Mechanical Engineering Department, Guararapes University Center, Piedade, Recife 54400-160

ARTICLE INFO

Article History:

Received 10th July, 2021

Received in revised form

14th August, 2021

Accepted 16th September, 2021

Published online 23rd October, 2021

Key Words:

AA3303, Aluminum Alloy, Al-Mn, Hot Extrusion, Powder Metallurgy.

*Corresponding author:

Ana Paula Muniz Serejo

ABSTRACT

This work's main objective was the manufacture of an aluminum alloy AA3303 by powder metallurgy technique and its characterization. The powders were processed by high energy ball milling (HEBM) for 30, 60 and 120 minutes and then characterized by scanning electron microscopy (SEM), dispersive energy spectroscopy (EDS), X-ray diffraction (XRD) and finally, Laser Diffraction granulometry. After the characterization of the powders, they were consolidated by cold uniaxial compaction, followed by hot extrusion. Finally, the microstructural characterization of the sintered samples was performed using SEM, the chemical composition of the material was analyzed using the EDS technique, and then the material was subjected to the Vickers microhardness tests, enabling the study of the hardness property obtained in the samples. He characterization of the powders submitted to HEBM showed that with increasing grinding time the median particle size decreased, reaching values very close to those found in commercial AA100 aluminum. The materials consolidated by hot extrusion showed a homogeneous microstructure and almost free of porosity, resulting in excellent hardness values and attesting to the mechanical quality of the samples consolidated by hot extrusion.

Copyright © 2021, Moisés Euclides da Silva Junior et al. This is an open access article distributed under the Creative Commons Attribution License, which permits unrestricted use, distribution, and reproduction in any medium, provided the original work is properly cited.

Citation: Moisés Euclides da Silva Junior, Diogo Monteiro do Nascimento, Enéas Carlos de Oliveira Silva, Inaldo Amorim da Silva et al. "Manufacturing and processing of AA3303 aluminum alloy by synthesis of elementary powders by powder metallurgy techniques of high energy ball milling and hot extrusion", *International Journal of Development Research*, 11, (10), 50668-50675.

INTRODUCTION

Although most of the metallic components manufactured are produced using ferrous alloys such as steel and cast iron, which cover the vast majority of commercial and industrial applications, alloys classified as non-ferrous have achieved considerable growth in their production and application in past decades. Among these non-ferrous alloys, aluminum alloys stand out and have been increasingly used in the aeronautical industry and components for the manufacture of automobiles (BARBOSA, 2014). Aluminum is one of the most used materials in the world, presenting considerable application in several sectors, and this is due to its characteristics. The manufacture of finished products, such as: sheets, plates, aluminum castings, cast and forged profiles, provides more and more effective solutions for its application in the industrial sector.

The association of elements of alloys, such as: magnesium, silicon, copper, manganese, iron and zinc, provides modifications in the characteristics of aluminum, thus enabling its application in several segments, such as: goods and consumption, automotive and transport, civil construction, packaging, machinery and equipment. Among these sectors the automotive and transport industry is the largest consumer of aluminum in the world (ABAL, 2019; CALLISTER; RETHWISCH, 2016). Placed in a highly competitive context, the automobile industry was one of the main responsible for the growth in the use of sintered components, manufactured through Powder Metallurgy - PM. Powder metallurgy is a technique for manufacturing components using powders, it is a process that can produce a large volume of aluminum components, with complex shapes and without the need for subsequent finishing operations. From an economic point of view, powder metallurgy has become irreplaceable due to its high productivity, a factor that is fundamental for the definition of the choice of the manufacturing method in modern industry

(CHIAVERINI, 2001; DANNINGER; CALDERON; GIERL-MAYER, 2017). In this context, the aforementioned work discusses the manufacture of the aluminum alloy of the AA3XXX series (AA3303), manufactured via powder metallurgy, by high energy ball milling (HEBM) and consolidated by pre-compaction and hot extrusion.

MATERIALS AND METHODS

Initially, the composition of the alloy to be manufactured according to the ASM Handbook (1992) was selected, with the percentages referring to each element of the alloys, the elemental powders were separated and then weighed on an analytical precision scale. Subsequently, these powders were subjected to High Energy ball milling (HEBM) through a SPEX type vibrating ball mill, for 30, 60 and 120 minutes. Then, both the particulate material of the AA3303 alloy processed by HEBM, and the pure aluminum alloy AA1100, and the Mn powder without HEBM processing were subjected to a size and particle analysis by laser diffraction.

The microstructural and chemical characterization of the particulate material was performed using the techniques of Scanning Electron Microscopy (SEM) and Energy Dispersive Spectroscopy (EDS), the study and identification of the phases generated after the HEBM was carried out through X-Ray Diffraction (XRD). The powders processed by HEBM, were consolidated through the pre-compaction process followed by hot extrusion. From the billet obtained by hot extrusion of the particulate material of the alloy under study, 3 specimens were manufactured and then the specimens were subjected to the metallographic preparation process (cutting, inlaying, grinding, polishing and chemical attack). The microstructural and chemical characterization of the hot-extruded consolidated material was performed using the techniques of scanning electron microscopy (SEM) associated with energy dispersive spectroscopy (EDS).

Finishing the characterization process of the consolidated material, the sintered and extruded specimens were subjected to a Vickers microhardness test, thus determining the hardness property of the studied material. Table 1, expressed as percentage compositions by weight for the aluminum alloys of the present study, according to ASM Handbook (1992).

Table 2 presents as mass prescriptions in (g), of each of the chemical elements that make up the aluminum alloys of the related study, which will be subjected to high energy ball milling. The mass percentages are in accordance with the ASM Handbook (1992). The mass submitted to HEBM was 20,000 (g), plus 1% of the PCA as indicated by De Araujo Filho *et al.* (2017), totaling 20,200 (g).

Table 1. Composition of AA3303 alloy

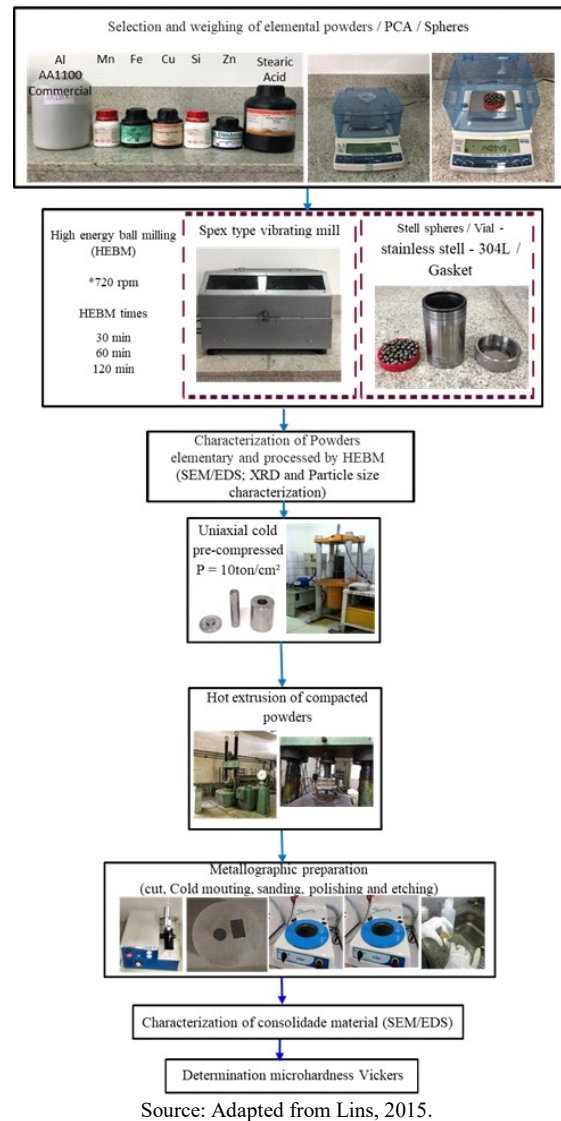
Aluminum Association	wt%					
	Si	Fe	Cu	Mn	Zn	Al
AA3303	0.60	0.70	0.20	1.50	0.30	96.70

Source: Adapted from ASM Handbook, 1992

Table 2. Composition of the powder mass and PCA by grinding time

Aluminum alloy	HEBM time (min)	Composition, (g)						
		Si	Fe	Cu	Mn	Zn	Al (1100)	PCA
AA3303	30	0.120	0.140	0.040	0.300	0.060	19.340	0.200
	60	0.120	0.140	0.040	0.300	0.060	19.340	0.200
	120	0.120	0.140	0.040	0.300	0.060	19.340	0.200

The Figure 1 schematically illustrates the process flow applied in this work, briefly presenting the work sequence.



High energy ball milling (HEBM): HEBM was performed in a Spex type vibrating mill, with 30, 60 and 120 minutes of duration. Ball-to-powder ratio (BPR) was used for a 10:1 ratio as indicated by Bezerra *et al.* (2014). It was performed a wet milling, using isopropyl alcohol as PCA. After milling the powders were dried in an oven at a temperature of 100°C.

X-ray diffraction (XRD): XRD tests were performed on SHIMADZU MAXIMA XRD-7000 equipment. The following parameters were used according to Nascimento *et al.* (2021)

- Diffraction angle: θ -2 θ ;
- Scan range: 25° - 120°;
- Scan mode: continuous scanning;
- Scan speed: 1°/min;
- Step: 0.01°/seg.

Granulometry: It was used the laser diffraction technique in liquid medium, using water as dispersant. The equipment used was the MALVERN INSTRUMENTES U.K. MASTERSIZER 2000.

Compaction and extrusion: The powders were uniaxial cold pre-compacted in a hydraulic press. A compaction pressure of 10 ton/cm² was used during 10 minutes. The extrusion was conducted at a temperature of 500 °C, a progressive extrusion pressure and a feed rate of 2 mm/s were applied (De Araujo Filho *et al.* 2017; Nascimento *et al.* 2021). Figure 2 shows aluminum alloy before and after extrusion.



Figure 2. Aluminum Alloy before and after extrusion

Samples preparation: Three samples of the extruded material were taken, and then the samples were sectioned into two sections: transverse (perpendicular to the direction of extrusion) and longitudinal (parallel to the direction of extrusion), according to the sample cutting plan illustrated in the Figure 3. The extruded samples were cut with a precision cutter STRUERS ACCUTOM-100.

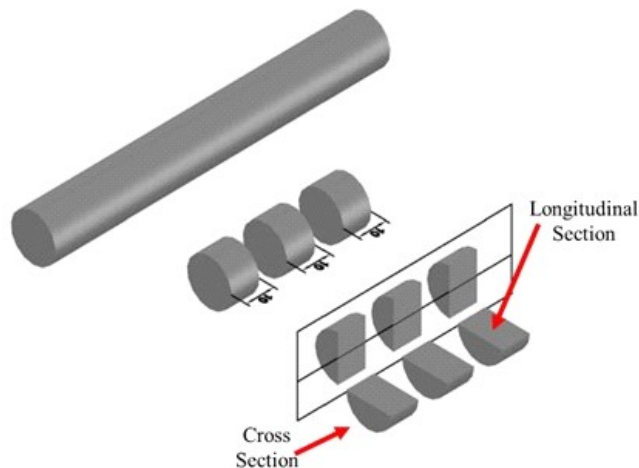


Figure 3. Sample cutting plan

Scanning electron microscopy (SEM): SEM and energy dispersive spectroscopy (EDS) were performed on the TESCAN MIRA3 microscope.

Microhardness Vickers: A load of 0.2 kgf was applied for 15 seconds according to Nascimento *et al.* (2021). The tests were performed on an EMCOTEST DURASCAN 700 durometer.

RESULTS AND DISCUSSION

Characterization of particulate material

X-ray diffraction (XRD): Figure 4, illustrates the X-ray diffraction pattern, obtained through the AA1100 aluminum powder as received, it presented only the characteristic aluminum peaks that were identified by the reference ICDD 03-065-2869 microfiches. When analyzing it, it shows the presence of only one crystalline phase belonging to aluminum, which is the centered face cubic phase (FCC). According to Callister and Rethwisch (2016), for this type of structure (FCC), the Miller indices (h, k, l) must be all even numbers or all odd numbers, as evidenced in the diffractogram illustrated in Figure 4. Figure 5 illustrates the X-ray diffraction pattern obtained through manganese, which showed only the characteristic peaks of manganese that were identified by the reference ICDD 01-071-0399 microfiches. The diffractogram shown in Figure 5 shows the presence of only one crystalline phase belonging to manganese, which is the centered body cubic phase (BCC). According to Callister and Rethwisch (2016), for this type of structure (BCC), the sum of the Miller indices (h + k + l) must be an even number, as evidenced in the diffractogram illustrated in Figure 5. Figure 6 shows the diffractograms of AA3303 alloy powders, submitted to MAE for periods of 30, 60 and 120 minutes respectively. The milling times of 30 and 60 minutes, did not show the characteristic phase of the AA3XXX series alloys, which is the $Al_6(Mn, Fe)$. The powders processed by HEBM during a time of 30 minutes, presented only the

phases Al and Mn, which were identified by the reference microfiche ICDD 03-065-2869 and 01-089-2105, respectively.

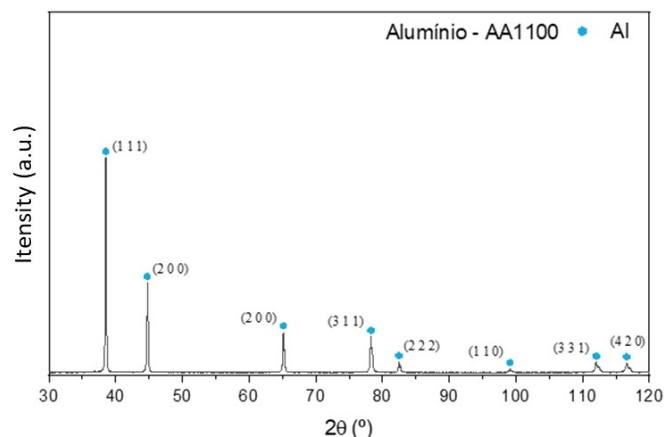


Figure 4 - X-ray diffraction pattern of AA1100 aluminum

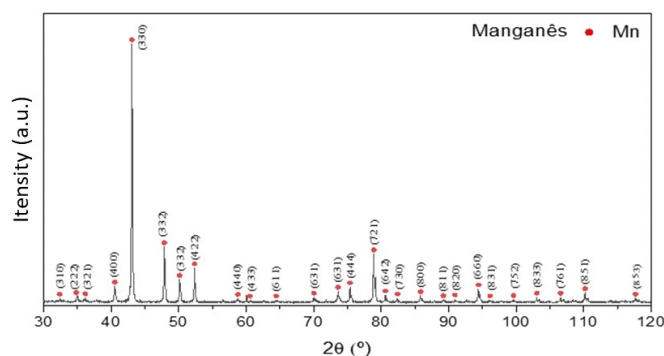


Figure 5. X-ray diffraction pattern of manganese

The powders processed by HEBM during a time of 60 minutes, presented only the phases Al and Mn, which were identified by the reference microfiche ICDD 03-065-2869 and 01-089-2105, respectively. The diffractogram of the powders processed by HEBM during 120 minutes, showed only the Al phase and the Al_6Mn phase, characteristic of the Al-Mn alloys, these phases were identified by the reference microfiche ICDD 03-065-2869 and 00-006-0665, respectively. The presence of the Al_6Mn phase only for the grinding time of 120 minutes, proves that the grinds of 30 and 60 minutes were not sufficient for the manufacture of the AA3303 alloy, by HEBM.

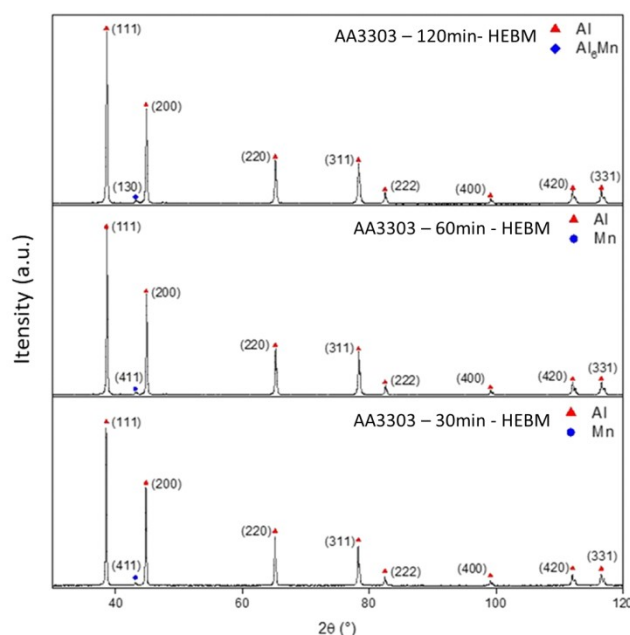


Figure 6. Diffraction pattern of AA3303 alloy powder, HEBM for 30, 60 and 120 minutes

Granulometry: Elementary powders, aluminum and manganese, were characterized both in terms of the type of particle size distribution and the average particle size through laser diffraction. The laser diffraction spectrum illustrated in Figure 7, refers to the granulometric analysis of the AA1100 aluminum powder as received, it shows a unimodal distribution, showing only a peak in the graphical representation, that is, the volumetric percentage is in just a range of values. For the aluminum powder AA1100 as received, the results of the granulometric analysis showed, with regard to the average diameter of the particles, that 10% d (0.1) of them are below 11.907 μm , 50% d (0.5) of them are below 28,992 μm and that 90% d (0.9) of them are below 64.026 μm . The laser diffraction spectrum illustrated in Figure 8, refers to the granulometric analysis of the manganese powder as received, it shows a unimodal distribution, showing only a peak in the graphical representation, that is, the volumetric percentage is found in only a range of values. For the manganese powder as received, the results of the granulometric analysis showed that with respect to the average diameter of the d medium particles, 10% d (0.1) of them are below 9.833 μm , 50% d (0.5) of them are below 24,034 μm and that 90% d (0.9) of them are below 52.232 μm .

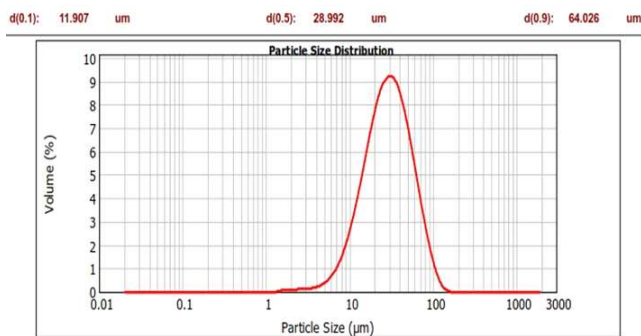


Figure 7. Laser diffraction spectrum of aluminum powder AA1100

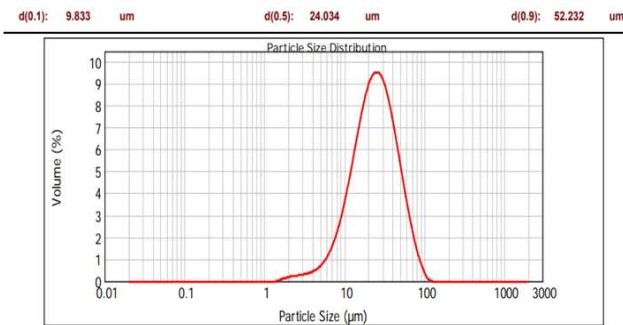


Figure 8. Laser diffraction spectrum of manganese powder

The AA3303 aluminum alloy powders processed by HEBM for 30, 60 and 120 minutes, were subjected to laser diffraction, and were characterized according to their particle size and particle size distribution. Figures 9, 10 and 11 illustrate the respective size distributions according to the grinding time.

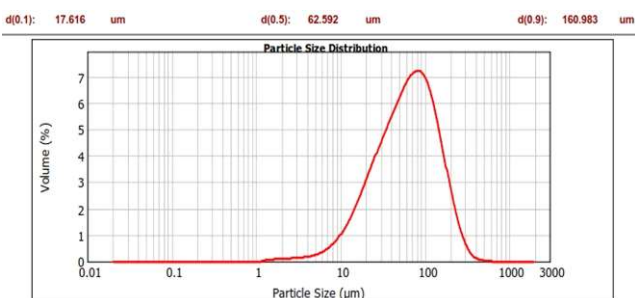


Figure 9. Laser powder diffraction spectrum of AA3303 alloy - 30 min. by HEBM

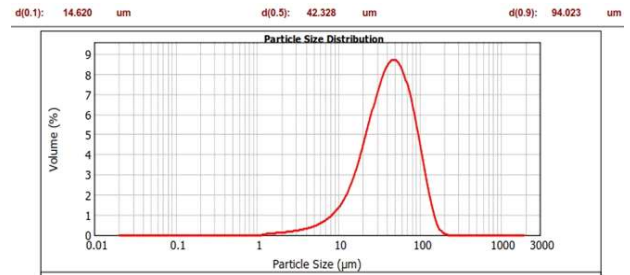


Figure 10. Laser powder diffraction spectrum of AA3303 alloy - 60 min. by HEBM

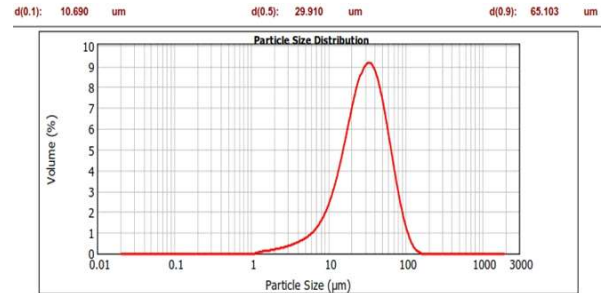
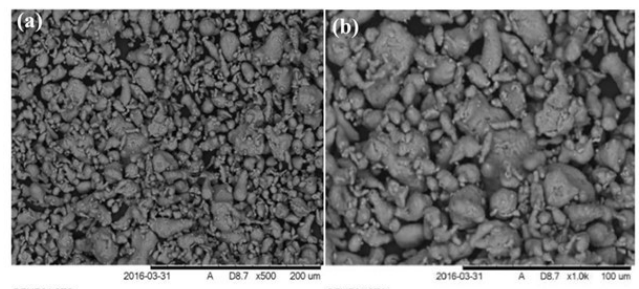


Figure 11. Laser powder diffraction spectrum of AA3303 alloy - 120 min. from by HEBM

Regarding the particle size distribution of the AA3303 aluminum alloy powders analyzed, it is possible to observe through Figures 9, 10 and 11 that the particulate material shows a unimodal distribution regardless of the HEBM time. For the aluminum alloy AA3303, the powder submitted to grinding during a period of 30 min, presented a median diameter d (0.5) of 62.592 μm , when compared with the average diameter of the starting powder of the aluminum alloy AA1100, this suggests that in this grinding time the phenomenon of cold welding was predominant, with the increase in the grinding time to 60 min, the material presented particles with a median diameter d (0.5) of 42.328 μm , this reduction in particle size shows that the phenomenon of fatigue fracture begins to overlap with that of cold welding. Finally, the material submitted to HEBM for a period of 120 minutes, presented a unimodal distribution and a median diameter of d (0.5) of 29.910 μm . When analyzing the evolution of the particle size, it is evident that with the increase of the grinding time the particle size reduced, thus obtaining with the HEBM during a period of 120min, a value very close to the average diameter of the starting powder of the alloy of AA1100 aluminum which is d (0.5) = 28.992 μm .

Scanning electron microscopy (SEM) and Energy Dispersive Spectroscopy (EDS): Figures 12 (a) and (b) are SEM micrographs referring to the aluminum powder of the AA1100 alloy as received, obtained by Silva (2017). When analyzing these images it is possible to identify a certain homogeneity of the particles, these micrographs also make it possible to verify that the powder has considerably small particles and a predominantly spherical morphology with grains with approximately axis-equal dimensions, thus evidencing that the material was obtained through the process of gas atomization as informed by the manufacturer.



Source: Silva, 2017

Figure 12. (a) SEM Al powder - AA1100 - 1000x; (b) SEM Al powder - AA1100 - 2000x

Figures 13 (a) and (b) are SEM micrographs referring to the manganese powder as received. Unlike what was observed in the AA1100 aluminum powder micrographs, the manganese powder micrographs show a non-homogeneous and quite irregular morphology, formed by flat grains with non-equiaxial dimensions, and with a particle size close to what was observed in the micrographs of aluminum.

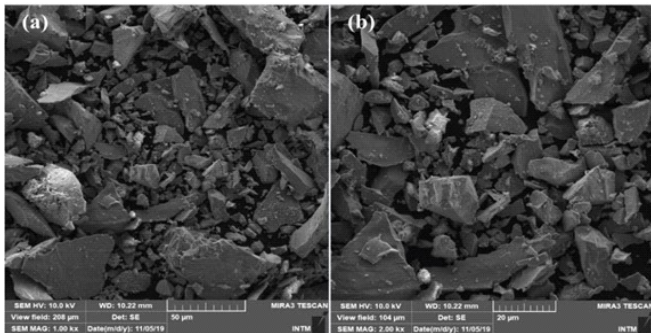
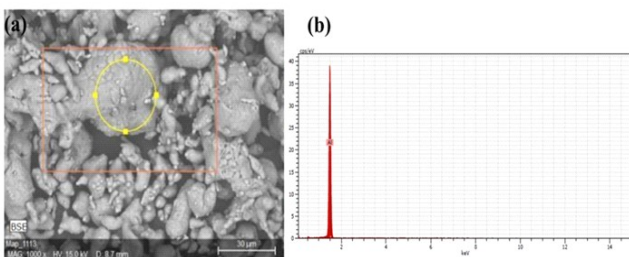


Figure 13. (a) SEM powder of Mn 1000x; (b) SEM powder of Mn 2000x

The SEM micrographs of aluminum and manganese powders make the normal and coherent aspects evident with regard to the morphology and granulometry of these materials. Figures 14 (a) and (b) were obtained by Silva (2017) and are respectively the analyzed region and the EDS spectrum, referring to the aluminum powder AA1100 as received. Although the equipment used provides only a semi-quantitative or qualitative analysis, the EDS spectrum obtained stands out for presenting only the aluminum peak, indicating that there was no contamination in the analyzed powder.



Source: Silva, 2017

Figure 14. EDS of Al AA1100; (a) Region analyzed; (b) EDS spectrum

Figures 15 (a) and (b), respectively, are the region analyzed and the spectrum of EDS referring to the manganese powder as received. The equipment used also provides a semi-quantitative analysis, but the analysis stands out indicating only the presence of manganese, thus proving that there was no contamination of the material.

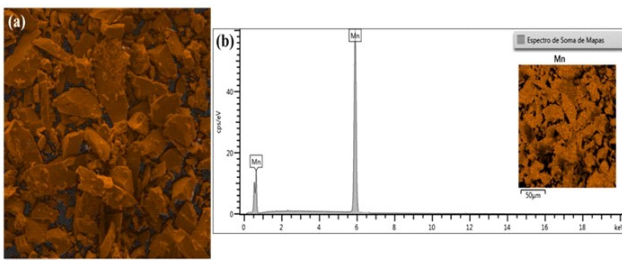


Figure 15. EDS of Mn; (a) Region analyzed; (b) EDS spectrum

Figures 16, 17 and 18 are SEM micrographs referring to the aluminum alloy AA3303, processed by HEBM for 30, 60 and 120min respectively. It is possible to observe that the samples of the AA3303 alloy, presented an irregular and flattened particle morphology, which according to Silva (2017) is a morphology that is in accordance with materials obtained by HEBM.

The micrographs of the aluminum alloy AA3303, also show that the increase in the grinding time contributed to the decrease of the particle size, producing particles with approximately the same shape and sizes.

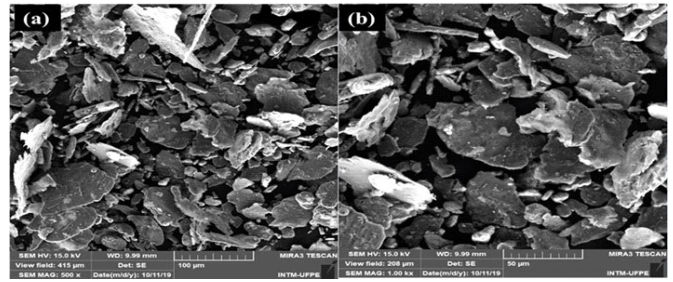


Figure 17. SEM micrograph of the AA3303 alloy - 60 min. MOM. (a) 500x magnification; (b) 1000x magnification

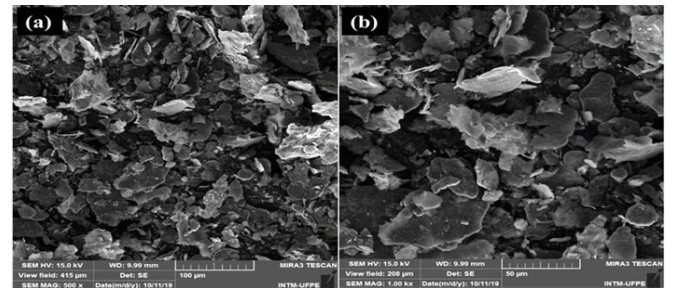
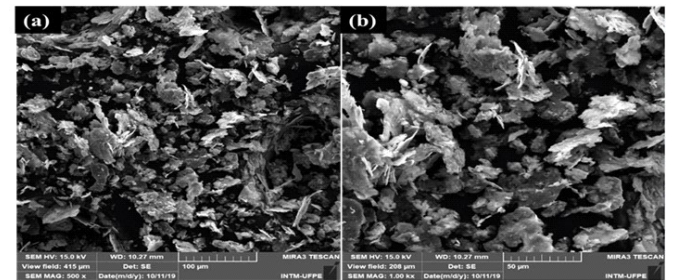


Figure 18. SEM micrograph of AA3303 alloy - 120 min. MOM. (a) 500x magnification; (b) 1000x magnification



Figures 19, 20 and 21 show the result obtained through the technique of dispersive energy spectroscopy, for characterization of the chemical compositions of the aluminum alloy AA3303 processed during 30, 60 and 120 minutes by HEBM. The results obtained through the analysis by EDS, for the alloy AA3303, show that regardless of the grinding time that it was submitted, the alloy under study presented only the chemical elements that constitute it, according to ASM Handbook (2001), which are: Al, Zn, Cu, Si, Mn and Fe. The images of the regions analyzed together with the help of the coloring referring to each chemical element, make it evident and facilitate the observation that the increase in the grinding time provides homogeneity in the distribution of the alloy elements. The presence of any chemical element that did not belong to the composition of the alloy was not found, thus characterizing that there was no contamination of the particulate material.

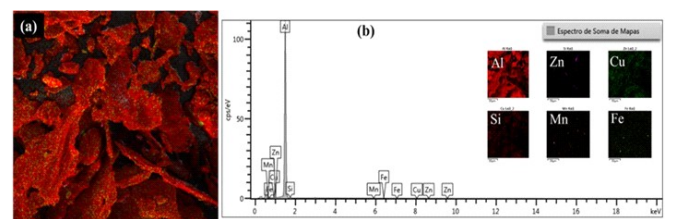


Figure 19. EDS AA3303 alloy powder map - 30 min. MOM; (a) Region analyzed; (b) EDS spectrum

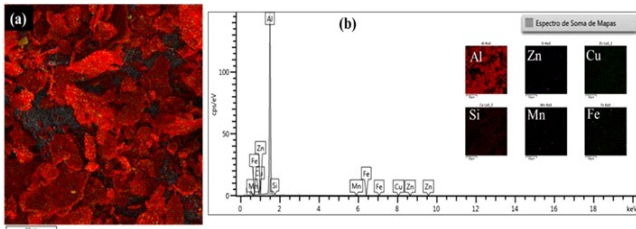


Figure 20. EDS AA3303 alloy powder map - 60 min. MOM; (a) Region analyzed; (b) EDS spectrum

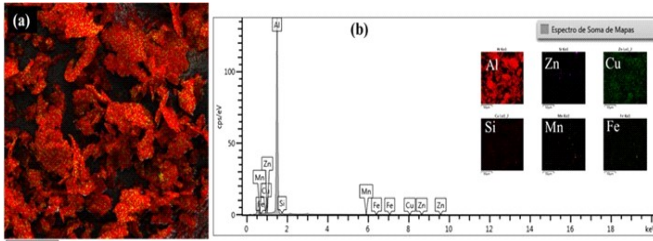


Figure 21. EDS AA3303 alloy powder map - 120 min. MOM; (a) Region analyzed; (b) EDS spectrum

Characterization of consolidated material: After characterizing the powders processed by high-energy ball milling for 30, 60 and 120 minutes, following the powder metallurgy manufacturing route, the particulate material was directed to the consolidation step. Only the powders of the samples processed by HEBM for 120 minutes were consolidated, due to the characteristic phase of the alloys of the Al-Mn system, the Al₆(Mn, Fe) phase and a smaller particle size. After the consolidation stage of the particulate material, the specimens obtained were submitted to the process of metallographic preparation and subsequent characterization. The consolidated material was characterized by SEM / EDS, and Vickers microhardness test.

Scanning electron microscopy (SEM) and Energy Dispersive Spectroscopy (EDS): Figures 22 (a, b, c and d) show SEM micrographs, referring to the transverse and longitudinal sections, of the hot extruded sample of the AA3303 alloy, with the 2000x and 5000x magnifications. The micrographs illustrated in the 22 (a, b, c and d), present a homogeneous microstructure with little porosity. Figures 23 and 25 shows the micro-analyses of point EDS of the cross-section and longitudinal section of the extruded sample of the AA3303 alloy. The light gray precipitates (indicated by the yellow circles) in Figures 22 (a, b, c and d), were identified in spectrum 7 of Figure 23 and in spectrum 17 of Figure 25, as a compound of Al and Si. Light colored precipitates (indicated by blue circles) were identified in spectrum 8 and 9 in Figure 23 and in spectrum 18 and 19 in Figure 25, as a compound of Al, Cu, Fe, Mn and Zn.

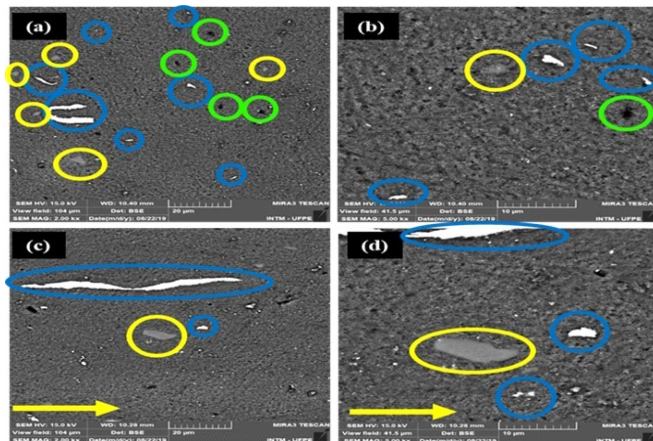


Figure 22 - SEM micrograph of the extruded alloy of the AA3303 alloy - 120 min. HEBM - cross section: 2000x (a), 5000x (b) - longitudinal section: 2000x (c), 5000x (d)

These precipitates have different sizes, mostly an elongated shape, mainly in the longitudinal section, where they are parallel to the direction of extrusion indicated by the yellow arrows. The EDS spectrum 10 of Figure 23, identifies a dark colored precipitate (indicated by green circles), as a compound of Al and Mn, the percentages of the elements suggest that this precipitate is from the orthorhombic phase Al₆Mn. Figures 23 and 26 respectively show the maps of the EDS analysis of the cross and longitudinal sections of the sample of the extruded AA3303 alloy. The EDS analyzes carried out in the transversal and longitudinal sections of the extruded sample of the alloy AA3303 identified only the chemical elements that make up the alloy, no contamination was identified.

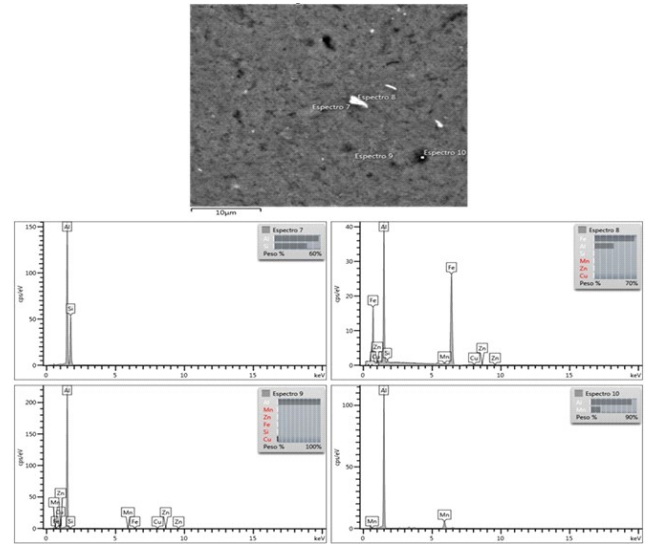


Figure 23. EDS spectrum of AA3303 alloy extrudate - 120 min. HEBM - cross section

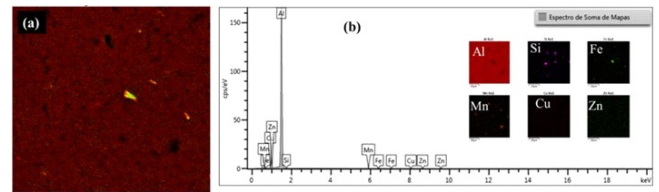


Figure 24. EDS map of AA3303 alloy extrudate - 120 min. MAE - cross section (a) Region analyzed; (b) EDS spectrum

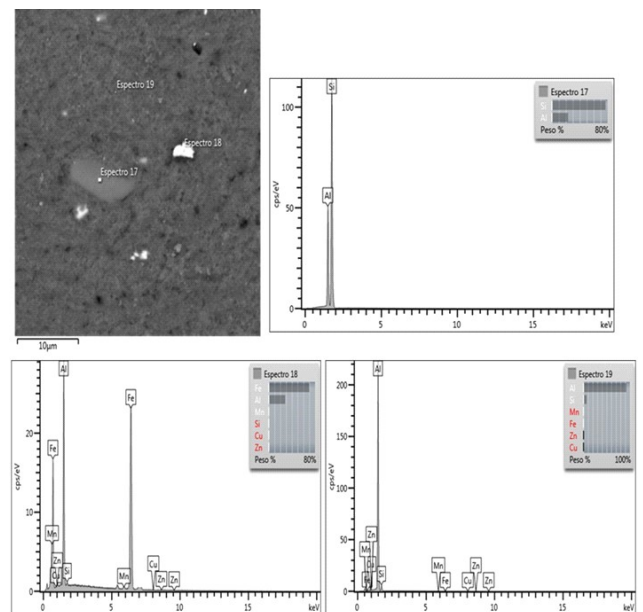


Figure 25. EDS spectrum of AA3303 alloy extrudate - 120 min. HEBM - longitudinal section

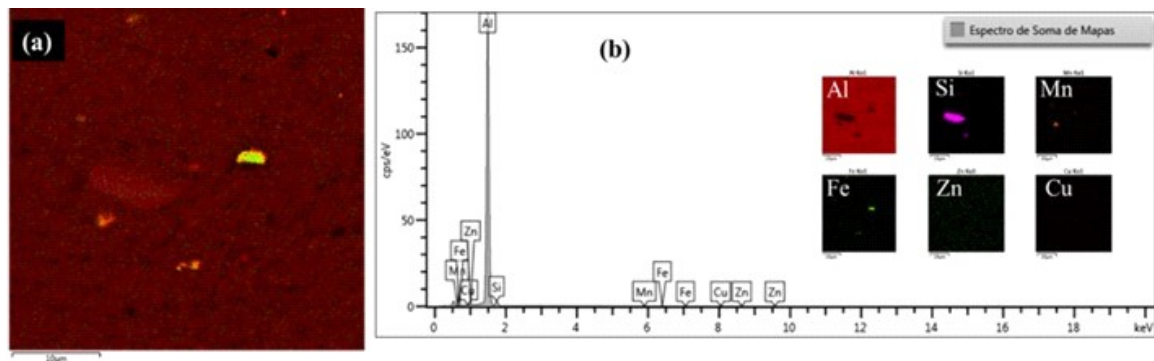


Figure 26. EDS map of AA3303 alloy extrudate - 120 min. MAE - longitudinal section (a) Region analyzed; (b) EDS spectrum

Table 3. Vickers microhardness test

Sample	Extruded					
	AA3303-1		AA3303-2		AA3303-3	
	Cross section	Longitudinal section	Cross section	Longitudinal section	Cross section	Longitudinal section
1 ^a Indentation	67.30	71.10	71.50	71.90	78.80	76.60
2 ^a Indentation	70.70	68.80	71.50	74.70	80.60	73.70
3 ^a Indentation	69.00	67.40	71.80	72.40	82.70	77.60
4 ^a Indentation	78.10	70.70	71.90	72.40	81.00	72.00
5 ^a Indentation	72.90	74.20	69.80	73.30	80.00	76.50
Average	71.60	70.44	71.30	72.94	80.62	75.28
Pattern deviation	3.74	2.31	0.77	0.99	1.28	2.09

Table 4 .Average Vickers microhardness test and Average pattern deviation

Sample AA3303	Cross section	Longitudinal section
General overall average	74.51	72.89
General pattern deviation	1.93	1.80

Vickers Microhardness Test of consolidated material: In order to assess the repeatability of the manufacturing process of the alloys manufactured using the powder metallurgy technique, three specimens of the extruded billet were manufactured, all 3 samples were subjected to the Vickers microhardness test, a load was used 0.2 kgf (HV0.2). Tables 1 shows the results of the 5 indentations performed on each of the 3 specimens and calculated average hardness. Martins and Padilha (2006) characterized the commercial aluminum alloy 3003 produced by continuous casting of sheets (twin roll caster), and obtained the following hardness values: gross casting 54 HV and 39.4 HV for the homogenized sample. No study on the characterization of the AA3303 alloy was found, but it is expected that it behaves in a similar way to the AA3003 alloy, since the percentages of the alloying elements (Si, Cu, Fe and Mn) are identical, varying only the percentage of Zn, which is 0.10% for the AA3003 alloy and 0.30% for the AA3303 alloy, according to ASM Handbook (1992). Table 3 shows the hardness values obtained in each of the 5 indentations made in each of the cuts (transversal and longitudinal) and the calculations of their respective average and pattern deviation. When compared with the samples extruded with the material with the material manufactured by Martins and Padilha (2006), the mechanical superiority of the specimens submitted to extrusion is notorious, as they obtained a considerable increase in hardness and lower values of standard deviation, this increase in hardness associated with lower pattern deviation values is justified by the higher densification of the material provided by the hot extrusion process, which according to Fogagnolo (2000) and Nascimento (2021), in aluminum powders provides a breakdown of the oxide layer that covers the particles, generating thus a greater connection between them, and eliminating the typical porosity of the sinter. material. According to Costa (1998), the extruded product has strong bonds between the particles that produce a final structure equivalent to that of a forged product. Table 4 shows the general average of the Vickers microhardness values and the average of the pattern deviations for each of the sections calculated from the data in Table 3.

CONCLUSION

The powder metallurgy technique was effective in the manufacture of the AA3303 alloy, and produced samples with excellent characteristics. The results of the analysis of granulometry by laser diffraction, showed the influence of the grinding time in the reduction of the particle size. The HEBM times of 30 and 60 minutes were not enough to manufacture the AA3303 alloy, as they were not enough to form the Al_6 (Mn, Fe) phase, characteristic of the AA3XXX series alloys, in addition they produced particle sizes much larger than those found in starting powders. Only in powders subjected to HEBM for 120 minutes, the orthorhombic phase Al_6 (Mn, Fe) was identified by X-ray diffraction, which is characteristic of the aluminum alloys composed by the Al-Mn system, thus characterizing the incorporation of alloy elements in the matrix and the formation of the alloy itself. In addition, the 120-minute milling produced median particle sizes very close to those found in the starting powders Al and Mn. The SEM results of the samples consolidated by hot extrusion showed a homogeneous morphology, with little or no porosity, a result that is characteristic of the hot extrusion process. The results of EDS indicated only the presence of the chemical elements that compose them, and the presence of a precipitate composed of Al and Mn, with percentages that correspond to the orthorhombic phase Al_6 (Mn, Fe), verifying that there was no contamination during the manufacturing process. The Vickers microhardness results of the hot-extruded samples show much higher hardness values associated with a very low pattern deviation. This is due to the hot extrusion process providing a plastic deformation in the powder particles, thus generating an increase in hardness to the material.

Acknowledgment

The authors wish to thank the Federal University of Pernambuco (UFPE), Mechanical Engineering Department, Pos-Graduate Program in Mechanical Engineering (GPME), CNPq, CAPES, INTM-UFPE and FACEPE.

REFERENCES

- ABAL. Associação Brasileira do Alumínio. Vantagens do Alumínio. Disponível em: <<https://abal.org.br/aluminio/vantagens-do-aluminio/>>. Acesso em: 15 mai. 2021.
- De Araujo Filho. O.O.; Araújo. Everthon Rodrigues de; Lira. Heronilton Mendes de; Gonzalez. Cezar Henrique; Silva. Noelle D'emery Gomes; Urtiga Filho. Severino Leopoldino. Manufacturing of AA2124 Aluminum Alloy Metal Matrix Composites Reinforced by Silicon Carbide Processed by Powder Metallurgy Techniques of High Energy Ball Milling and Hot Extrusion. Materials Science Forum. [S.L.]. v. 899. p. 25-30. jul. 2017. Trans Tech Publications. Ltd.. <http://dx.doi.org/10.4028/www.scientific.net/msf.899.25>.
- ASM Handbook. Properties and Selection: Nonferrous Alloys and Special-Purpose Materials. ASM International (American Society for Metals). Materials Park. Ohio. USA. 1992. v. 2. 3470 p.
- Barbosa. C. Metais não ferrosos e suas ligas: microestrutura, propriedades e aplicações. Rio de Janeiro: E-papers. 2014. 532 p.
- Bezerra. Carlos Augusto; Moura. Alexandre Douglas Araújo de; Araújo. Edval Gonçalves de; Santos. Maurílio José dos; De Araujo Filho. O.O. Features of the Processing of AA2124 Aluminum Alloy Metal Matrix Composites Reinforced by Silicon Nitride Prepared by Powder Metallurgy Techniques. Materials Science Forum. [S.L.]. v. 802. p. 108-113. dez. 2014. Trans Tech Publications.Ltd.. <http://dx.doi.org/10.4028/www.scientific.net/msf.802.108>
- Callister. W. D.; rethwisch. D. G. Ciência e Engenharia de Materiais: Uma introdução. 9. ed. Rio de Janeiro: LTC. 2016. 912 p.
- Chiaverini. V. Metalurgia do Pó. São Paulo: ABM. 2001. 334 p.
- Danninger. H.; calderon. R. O.; Gierl-Mayer. C. Powder Metallurgy and Sintered Materials. Ullmann's Encyclopedia Of Industrial Chemistry. [s.l.]. p.1-57. 30 nov. 2017. Wiley-VCH Verlag GmbH & Co. KGaA. Disponível em; http://dx.doi.org/10.1002/14356007.a22_105.pub2. Acesso em: 01 out. 2019.
- De Araujo Filho O. O.. De Araújo E. R.. De Lira H. M.. Gonzalez C. H.. Silva N. D. G.. Urtiga Filho S. L. (2017) Manufacturing of AA2124 Aluminum Alloy Metal Matrix Composites Reinforced by Silicon Carbide Processed by Powder Metallurgy Techniques of High Energy Ball Milling and Hot Extrusion. In Mater Sci Forum. 899. pp. 25-30.
- Lins. A. E. P. Fabricação de Compósitos de Matriz Metálica da Liga de Alumínio AA1100 com Reforço Cerâmico de Óxido de Zinco Através de Técnicas de Metalurgia do Pó. 2015. 114 f. Master Dissertation - Mechanical Engineering - Federal University of Pernambuco. Recife. 2015.
- Martins. J. P.; Padilha. A. F. Caracterização da liga comercial de alumínio 3003 produzida por fundição contínua de chapas (twin roll caster) - microestrutura. Metalurgia & Materiais. Ouro Preto. v. 59. n. 4. p.427-431. dez. 2006.
- Nascimento. D. M.; Silva Junior. M. E.; Costa. J. E. B.; Zarzar. S. T.; Muniz. M. B. B.; De Araujo Filho. O. O.. Manufacture and characterization of AA6061 aluminum alloy metal matrix composites with ceramic particulate reinforcement. International Journal of Development Research. [S.L.]. v. 11. p. 46875-46883. mai. 2021. <http://dx.doi.org/10.4028/www.scientific.net/msf.899.25>.
- Silva. T. T. L. Manufatura e caracterização de Alumínio-Cobre (Duralumínio) fabricadas via técnicas de metalurgia do pó. Master Dissertation - Mechanical Engineering - Federal University of Pernambuco. Recife. 2017.
